ELSEVIER

Journal of Nuclear Materials 258–263 (1998) 1687–1693

journal of nuclear materials

Low activation austenitic Mn-steel for in-vessel fusion materials

Y. Suzuki *, T. Saida, F. Kudough

Mitsubishi Heavy Industries, Ltd, Minatomirai, 3-Chome, Nishi-ku, Yokohama 220-8401, Japan

Abstract

Several compositions of austenitic manganese steels (Mn-steels) were investigated for in-vessel component materials in D–T fueled fusion reactor with respect to radiation exposure and waste disposal management. The 24.5Mn–13.5Cr steel was developed in which undesired impurities, such as Ni, Mo, Nb and Co, were controlled and C (∼0.025wt%) and N (∼0.22wt%) contents were well adjusted for corrosion resistance and weldability. Experimental observation has shown that this steel has a single γ-phase structure and good properties for vacuum vessel almost the same grade as Type 316 stainless steel (316SS), such as low permeability, good weldability, good mechanical properties of strength and toughness and good corrosion resistance. Activation calculations were performed adopting this material for the JT-60 Super Upgrade (JT-60SU) vacuum vessel and the effectiveness of low activation was confirmed.

1. Introduction

The fusion research has advanced to an engineering stage on which the D–T fueled experiments are performed. The D–T reaction produces 14 MeV neutrons, and the structural materials around the plasma are severely irradiated by neutron and charged particle radiation. This led to study of low activation materials for fusion components from both aspects of radiation exposure and waste disposal management. Type 316 stainless steel (316SS) is considered as an attractive structural material for the vacuum vessels of various fusion reactors, because of its excellent fabricability, mechanical properties, weldability and corrosion resistance, and so on. However, commercially available 316SS contains Ni, Mo and Co that cause such problem as long-life activation. Therefore, adjustment of alloying elements is required for vacuum vessel materials.

One of the attractive low activation steels is the austenitic Mn-steel from the view point of waste disposal because of few long-lived nuclides. Piatti et al., have investigated various types of low activation austenitic stainless steel based on Mn–Cr non-magnetic steels [1–4]. However, those alloys still have small amounts of Ni, Mo etc. We have conducted studies on high Mn–Cr steels to eliminate such undesirable elements and to develop lower activation austenitic stainless steels that meet the requirements for vacuum vessel materials of fusion reactor, such as low permeability, good mechanical weldability, good properties and good corrosion resistance. The detailed results will be separately reported [5].

In this paper, we describe the benefits of 24.5Mn–13.5Cr steel with no Ni for use as in-vessel fusion materials. The chemical compositions and characteristics of several Mn-steels are summarized in Section 2. The results of screening tests for these Mn-steels and the selection of candidate material are discussed in Section 3. In Section 4, activation characteristics of the 24.5Mn–13.5Cr steel are examined through activation calculations when adopting this steel to the JT-60 Super Upgrade (JT-60SU) vacuum vessel.

2. Chemical compositions and characteristics of candidate Mn-steels

In order to meet the requirements for vacuum vessel materials, adjustment of alloying elements in the stainless steels has been conducted as follows:

---

* Corresponding author. Tel.: +81 3 3218 2047; fax: +81 3 3211 3123; e-mail: yutaka@atom.hq.mhi.co.jp.

0022-3115/98/$19.00 © 1998 Elsevier Science B.V. All rights reserved.
PII: S0022-3115(98)00283-9

1. Elements of long-life activation, such as Ni, Mo, Nb, Al and Co, were eliminated. Since Ni is the strongest austenite stabilizer, careful adjustment of other elements is required to stabilize the austenite structure.
2. Mn is an important element to stabilize the austenite structure. However, an excess amount of Mn accelerates the production of intermetallic compounds and reduces ductility and corrosion resistance. Therefore, Mn was limited between 15% and 25%.
3. Although C is useful as an austenite stabilize, it reduces corrosion resistance. C was limited up to 0.1%.
4. N also functions as an austenite stabilizer. But as it reduces weldability, it was limited to less than 0.2%.
5. A content of more than 12% Cr improves corrosion resistance and increases nitrogen solubility. On the other hand, an excess amount of Cr destabilizes the austenite structure; therefore, it was limited in the range of 12–20%.
6. Reduction of strength caused by the decreased amounts of C and N can be compensated by an addition of V, which serves as a grain refining element. However, since an excess of V reduces weldability, V was restricted to 0.3% or less.

The development of the Mn–Cr based stainless steels was done considering the above factors. Five types of steels are proposed and their compositions along with those of the conventional 316SS are summarized in Table 1.

Alloys No. A and B are steels based on conventional 18Mn–18Cr and 15Mn–17Cr austenitic stainless steels, respectively, with reduced C and N contents to improve corrosion resistance and weldability [6,7]. Mn was further added to the No. B alloy to form No. C and D alloys. Furthermore, V is added to No. D to compensate the reduction in strength. For alloys No. E, the Cr content was reduced than No. C alloy in order to stabilize the austenite structure. Alloy No. F is a conventional 316SS, which was provided for comparison with these newly developed alloys. Ingots of about 50 kg of each of these alloys were fabricated by the vacuum high frequency induction furnace.

3. Screening tests for application to in-vessel materials

Screening tests of chemical composition, microstructure, and permeability etc. have been conducted on the fabricated alloys to identify the alloys with a single phase austenite structure. In addition, optimal conditions for solution heat-treatment were evaluated.

Examination of microstructures revealed that an austenitic single phase structure was obtained for alloys No. E and F. Fig. 1 shows the microstructure of alloy No. E for solution treated at 1050°C. Alloys No. A–D showed duplex structure with austenite phase, and mainly intermetallic compounds (such as σ-phase), carbide and δ-ferrite phase.

Permeability and δ-ferrite content were measured for alloys No. A–F to examine their magnetic properties. No ferrite was found in alloys No. E and F, confirming that they are fully austenite. High permeability and ferrite content were observed in alloys No. A–D.

The screening tests showed that only No. E alloy was a suitable candidate for non-magnetic stainless steels. To investigate the applicability of the alloy for vacuum vessel materials, a wide range of material tests have been conducted, including those of mechanical, thermal and magnetic properties, as well as characteristics of corrosion resistance. In addition, welded joints of the alloy have been evaluated. The material properties of the developed alloy were compared with those of 316SS (No. F).

Tensile properties, i.e., 0.2% yield strength, ultimate tensile strength and elongation of the alloy were mea-

Table 1
Designed/evaluated chemical composition and microstructure of the alloys

No	Composition	C	Si	Mn	P	S	Ni	Cr	Mo	V	N	Co	Micro-structure
A	Nominal	0.02	0.40	19.5	0.025	0.003	–	19.5	–	–	0.20	<0.03	γ + X
	Effective	0.021	0.30	19.33	0.027	0.007	0.02	19.43	0.01	<0.01	0.212	0.002	
B	Nominal	0.02	0.50	15.5	0.025	0.003	–	17.0	–	–	0.20	<0.03	γ + X
	Effective	0.023	0.47	15.30	0.025	0.007	0.01	16.93	0.01	0.01	0.202	<0.005	
C	Nominal	0.02	0.50	24.5	0.025	0.003	–	17.0	–	–	0.20	<0.03	γ + X
	Effective	0.026	0.47	24.67	0.027	0.010	0.01	17.10	0.01	<0.01	0.209	0.003	
D	Nominal	0.02	0.50	24.5	0.025	0.003	–	17.0	–	0.20	0.20	<0.03	γ + X
	Effective	0.024	0.48	24.50	0.027	0.006	0.01	17.09	0.01	0.20	0.209	0.002	
E	Nominal	0.02	0.50	24.5	0.025	0.003	–	13.5	–	–	0.20	<0.03	γ
	Effective	0.025	0.51	24.60	0.025	0.007	0.03	13.40	0.01	<0.10	0.219	0.003	
F (316SS)	Nominal	0.05	0.50	1.4	0.015	0.003	12.5	17.0	2.5	–	0.04	<0.03	γ
	Effective	0.039	0.50	1.49	0.017	0.006	12.57	17.49	2.56	<0.01	0.0432	<0.01	

Note: Chemical compositions were evaluated as mass% from the forged ingot. Microstructure was observed after the 1050°C solution heat treatment. γ: Austenite phase, X: Other phases except for γ.

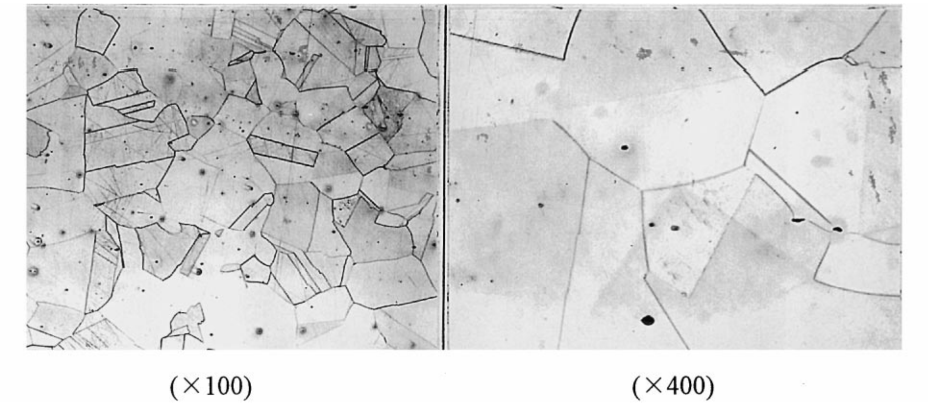

Fig. 1. Microstructure of alloy No. E (24.5Mn–13.5Cr with no Ni steel) at the solution treatment temperature of 1050°C. No ferrite was found and a single γ-phase structure was observed.

sured at a room temperature of 20°C and at an elevated temperature of 300°C. Results are summarized in Fig. 2. The tensile and yield strengths for No. E alloy and 316SS show an inverse temperature dependence. Although both of the alloys have similar levels of tensile properties at each temperature, ultimate tensile strength of No. E is larger than that of 316SS at room temperature.

The soundness of the welded joints of the alloy No. E and F has been evaluated using the electron beam (EB) welding method. No defects, such as cracks and cavities, were found in the welded joints of either alloy.

Tensile properties obtained for the welded joints are shown in Fig. 2. The 0.2% yield strength of the welded joints for No. E and F alloys was slightly increased. The ductility of the weld metals at room temperature was somewhat reduced for No. F alloy.

Various types of corrosion tests have been conducted. The results of general corrosion tests showed that, although the newly developed alloy had a good resistance against intergranular corrosion, its resistance against general and pitting corrosion was not as high as that of 316SS as shown in Table 2. However, the above corrosion tests were conducted under an extremely corrosive environment compared with the actual environment in a fusion reactor vacuum vessel. To further investigate the applicability of the developed alloy for fusion reactors, test specimens were exposed to a 19.1% H_3BO_3 water that was pressurized at 0.5MPa at 80°C for a month in order to simulate actual environmental conditions found in a vacuum vessel, which is cooled by H_3BO_3 water. The general and crevice corrosion rates were measured. In addition, susceptibility of the alloy to SCC was examined using a double U-bend test specimen. The developed alloy has a corrosion rate as low as that of 316SS. Also, no crack was observed in the two alloys after SCC tests. It is concluded that no significant inferiority in corrosion resistance exists in the developed alloy when compared with 316SS in an actual environment.

The corrosion test using 19.1% H_3BO_3 pressurized water was also performed for a month to the welded joints. The results are also presented in Table 2. It was found that both alloys had low corrosion rates for general corrosion and crevice corrosion. Susceptibility of the alloys to SCC was also shown to be negligible.

4. Activation calculations of 24.5Mn–13.5Cr steel

The low activity characteristics of the 24.5Mn–13.5Cr steel was examined for use with the JT-60SU vacuum vessel. The JT-60SU, which is proposed by JAERI, is designed utilizing as much construction of the existing JT-60U facility as possible [8,9]. The maximum neutron production rate is about 1×10^{18} s^{-1} and approximately 4×10^{22} D–D fusion neutrons per year are expected in JT-60SU [10]. The D–D neutron flux reaches about 1×10^{18} $s^{-1}cm^{-2}$ on the vacuum vessel surface. In this device, 10 years of D–D fueled experiment will be performed in its first stage of operation. At the second stage, 2 years of D–T operation is optionally planned.

The vacuum vessel is of double thin-wall water tank type construction, filled with shielding water within the tank. This concept was devised for the vacuum vessel of SSTR [11] and also planned to apply to that of ITER. For D–T optional operation, the additional shielding structures protecting the super-conducting magnet (SCM) are installed inside the vacuum vessel after 10-year D–D operation and 1-year cooling down period. This minor upgrade will have to be conducted inside the vacuum vessel under radioactive circumstances. Allowable limits of the biological shielding are designed as follows: (1) in vessel, about 100 μSv/h at 1 year after

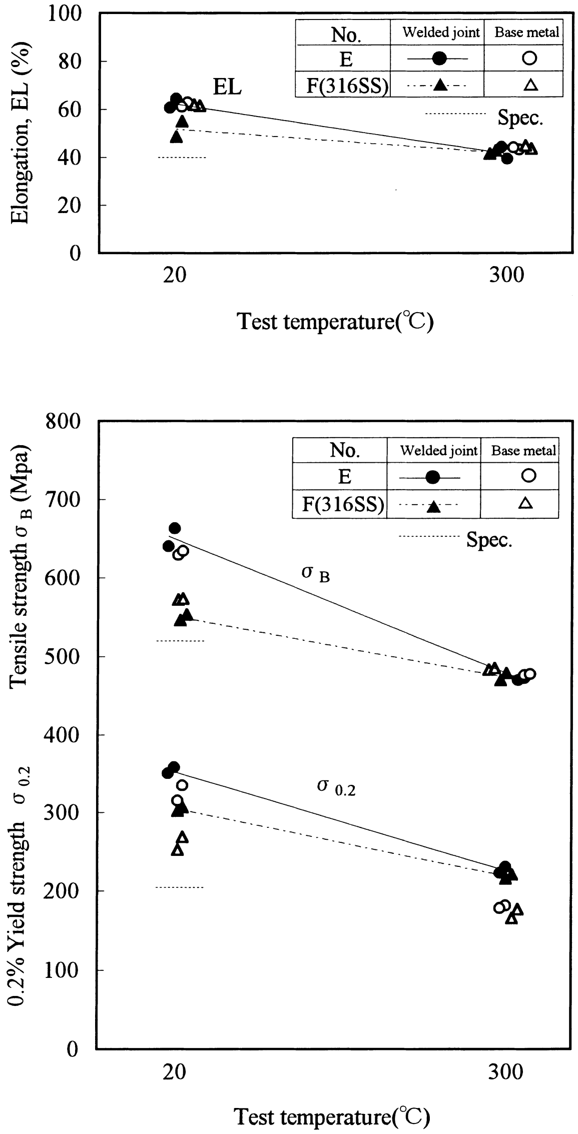

Fig. 2. Tensile properties of alloys.

shutdown; (2) in cryostat, about 20 μSv/h at 1 month after shutdown. For the nuclear heating rate in the SCM, an allowable limit of about 0.2 mW/cc is applied in the operation phase. The tungsten-shielding blocks are installed on the inner surface of the vacuum vessel as the internal liners for achievement of these requirements.

A one-dimensional activity calculation using THIDA-2 code system [12] was performed to calculate the induced radioactivity and the dose rate during the machine shutdown. Neutron and γ-ray transports and nuclear heating during operation were calculated by ANISN code [13]. The adopted nuclear group constant set was FUSION-40 [14]. The results of activation calculations for commercially available 316 SS (Case A: Co content is approximately 0.2 wt%), 316 SS with low-Co (Case B: 0.05 wt%) and 24.5Mn–13.5Cr steel (Case C) are shown in Fig. 3(a)–(c), respectively. In Case A, the maximum dose rate inside the vessel reached about 700 μSv/h, which was not allowable for human accessibility. In spite of the reduction of Co content in 316 SS, in Case B, the maximum dose rate inside the vessel was about twice of the allowable limit. The radioactive cooling time over 5 years was required to satisfy the condition. By adopting the 24.5Mn–13.5Cr steel for the vacuum vessel, in Case C, the γ-ray dose rate inside the vessel was below 100 μSv/h with 1 year cooling time after 10 years of D–D

Table 2
Corrosion test results of the alloys

Test case		Base metal							Welded joint [d]		
		General corrosion tests				Tests under actual environment [c]					
		10% oxalic acid etch test	Copper sulfate/ sulfuric acid test	5% sulfuric acid test	Ferric chlorite test	General corrosion	Crevice corrosion	Stress corrosion cracking	General corrosion	Crevice corrosion	Stress corrosion cracking
Evaluation item		Etch-structure at grain boundary	Damage	Corrosion rate (g/m^2 h)	Corrosion rate (g/m^2 h) 35°C/15°C	Corrosion rate (g/m^2 h)	Corrosion rate (g/m^2 h)	Damage	Corrosion rate (g/m^2 h)	Corrosion rate (g/m^2 h)	Damage
E	As SLT [a]	Dual (Partial ditch)	No crack	1021.7 1000.9	267.9 181.5	<0.6 <0.6	<1.0 <1.0	No crack	<0.6 <0.6	<1.0 <1.0	No crack
	Sensi-tized [b]	Ditch	Crack	1079.51021.9	256.5178.4	–	–	–	–	–	–
F(316SS)	As SLT [a]	Step (No ditch)	No crack	41.9 42.0	1.36 0.007	<0.6 <0.6	<1.0 <1.0	No crack	<0.6 <0.6	<1.0 <1.0	No crack
	Sensi-tized [b]	Ditch	Crack	176.3 200.9	12.7 2.2	–	–	–	–	–	–

[a] Samples were solution heat-treated at 1050°C × 1 h and water quenched.

[b] Samples were sensitized at 650°C × 2 h and air cooled.

[c] After 19.1% H_3BO_3 at 80°C × 1 month.

[d] Weld by electron beam.

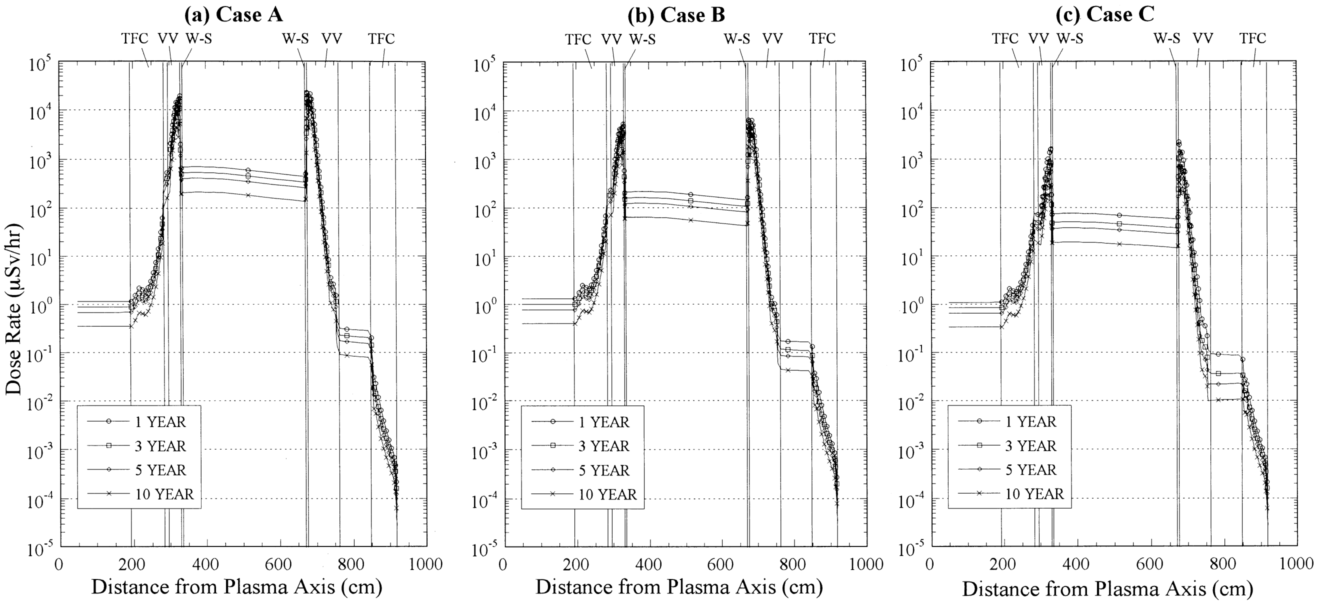

(a) Case A

(b) Case B

(c) Case C

Fig. 3. Shutdown γ-ray dose rate after 10 years' D–D operation. Case A: 316SS(0.2%Co), Case B: 316SS(0.05%Co), Case C: 24.5Mn-13.5Cr (TFC: toroidal field coil, VV: vacuum vessel, W–S: tungsten shielding).

operation as shown in Fig. 3(c). This amount of activity is acceptable for the accessibility into the vacuum vessel. At the same location, the γ-ray dose rate after 2 years of D–T operation will become less than 100 μSv/h for 20 years of cooling time. These results showed the superior low-activation property of this steel and found beneficial to waste disposal implications. The nuclear heating rate in the SCM is below 0.2 mW/cc in all cases.

5. Conclusions

We have investigated several compositions of austenitic manganese steels for use with the in-vessel components with respect to radiation exposure and waste disposal management. The major results in this work are summarized as follows:

1. From the results of the screening tests, we have developed the 24.5Mn–13.5Cr steel in which undesired elements for activation such as Ni, Mo, Nb and Co have been eliminated and C (~0.025 wt%) and N (~0.22 wt%) contents have been reduced for improving corrosion resistance and weldability.
2. This steel has a single γ-phase structure and good properties for use with the in-vessel components almost the same grade as 316SS, such as low permeability, good weldability, good mechanical properties of strength and toughness and good corrosion resistance.
3. From the activation calculations, in which this steel was used as the vacuum vessel material of JT-60SU, we confirmed that the γ-ray dose rate inside the vessel was below 100 μSv/h for the both case of 1 year cooling after 10 years of D–D operation and 20 years cooling after 2 years of D–T operation.
4. In conclusion, the 24.5Mn–13.5Cr steel developed in this work, appears to be effective candidate material for in-vessel materials in a fusion reactor considering that it is an extremely low activation structural material with comparable material properties to those of 316SS. To confirm its applicability, further investigations will be required, including the production on a plant scale. In addition, finer adjustment of the alloying elements and impurity control could further reduce the radioactivity and improve the physical and mechanical properties and corrosion resistance.

Acknowledgements

The authors would like to acknowledge Mr. K. Hamada in Mitsubishi Heavy Industries, LTD. (MHI) for his kind encouragement. They wish to thank Dr. M. Kikuchi, K. Ushigusa and members of the JT-60SU group in Japan Atomic Energy Research Institute (JAERI) for their helpful suggestion. They also wish to express their gratitude to Dr. M. Kusuhashi in Japan Steel Works, LTD. (JSW) for continued discussion and support.

References

[1] G. Piatti, S. Matteazzi, G. Petrone, Nucl. Eng. Design/ Fusion 2 (1985) 391.

[2] G. Piatti, P. Schiller, J. Nucl Mater. 141–143 (1986) 417.

[3] G. Piatti, D. Boerman, J. Heritier, Proceedings of the 15th Symposium Fusion Technology, 1988, p. 983.

[4] M. Zucchetti, M. Zublena, Proceedings of the 15th Symposium Fusion Technology, 1988, 991.

[5] M. Onozuka, T. Saida et al., J. Nucl. Mater., to be submitted.

[6] K. Orita, Y. Ikeda, T. Iwadate, J. Ishizaka, ISIJ International 30 (1990) 587.

[7] K. Ohnishi, R. Miura, H. Tsukada, K. Sekimura, H. Moritani, A. Fuji, JSW Tech. Rev. 40 (1981) 12 (in Japanese).

[8] M. Kikuchi, K. Nagashima, T. Aoyagi et al., Proceedings of the 16th Symposium Fusion Engineering, IL, 1995, p 650.

[9] M. Kikuchi, N. Miya, K. Ushigusa et al., Proceedings of the 16th IAEA Fusion Energy Conference, IAEA-CN-64/ 62-3, 1996.

[10] N. Miya, T. Hayashi, Y Suzuki et al., Fusion Eng. Design 36 (1997) 309.

[11] Y. Seki, H. Iida, H. Kawasaki et al., THIDA-2: An advanced code system for calculation of transmutation, activation, decay heat and dose rate, Report JAERI 1301, 1986.

[12] W.W. Engle Jr., A user's manual for ANISN, K-1693, 1967.

[13] K. Maki, K. Kosako, Y. Seki et al., Nuclear group constant set FUSION/J3 for fusion reactor nuclear calculations based on JENDL-3 (in Japanese), Report JAERI-M 91-072, 1991.

[14] Y. Suzuki, M. Yamada, M. Tomita et al., Fusion Eng. Design 18 (1991) 209.